35th Annual International Conference of the IEEE EMBS
Osaka, Japan, 3 - 7 July, 2013

Parametric Imaging via Kinetics-Induced Filter for Dynamic Positron Emission Tomography

Zhaoying Bian, Jing Huang*, Lijun Lu, Jianhua Ma, Dong Zeng, Qianjin Feng, and Wufan Chen

***Abstract*— Due to the noisy measurement of the voxel-wise time activity curve (TAC), parametric imaging for dynamic positron emission tomography (PET) is a challenging task. To address this problem, some spatial filters, such as Gaussian filter, bilateral filter, wavelet-based filter, and so on, are often performed to reduce the noise of each frame. However, these filters usually just consider local properties of each frame without exploring the kinetic information. In this paper, aiming to improve the quantitative accuracy of parametric imaging, we present a kinetics-induced filter to lower the noise of dynamic PET images by incorporating the kinetic information. The present kinetics-induced filter is designed via the similarity between voxel-wise TACs under the framework of bilateral filter. Experimental results with a simulation study demonstrate that the present kinetics-induced filter can achieve noticeable gains than other existing methods for parametric images in terms of quantitative accuracy measures.**

I. Introduction

Dynamic positron emission tomography (PET) is a powerful tool in studying the physiological and biological processes of radiopharmaceuticals within human body [1]. To investigate the useful information from dynamic PET imaging, parametric images should be calculated through fitting time activity curves (TAC) at each voxel with a linear or nonlinear kinetic model [2]. However, due to finite spatial resolution of PET scanners and low signal to noise ratio (SNR) in short dynamic frames, some noticeable errors are inevitable transferred to the voxel-wise kinetic parameter imaging from the associative noisy TAC measurements.

To improve the quality of parametric images, many efforts have been done to reduce the noise of the dynamic PET images using image post-processing techniques, such as Gaussian filter, bilateral filter, wavelet-based filter, and so on [3-6]. Among these techniques, a simple and commonly used strategy is Gaussian filter. Extensive experiments show that Gaussian filter preforms well in the homogeneous region with noticeable noise reduction, but fails at edges with spatial resolution loss due to its shift invariance. As an extended version of Gaussian filter, bilateral filter was investigated in PET studies with significant gains than Gaussian filter in terms of the noise reduction and resolution preservation [6]. However, it is worth to note that all these spatial filter methods just reduce the noise in individual frames without considering the kinetic information contained within all the dynamic images.

In this paper, aiming to improve the quantitative accuracy of parametric imaging, we develop a kinetics-induced filter to lower the noise of dynamic PET images by incorporating the kinetic information. The present kinetics-induced filter is designed via the similarity between voxel-wise TACs under the framework of bilateral filter because the tendency of the TAC can provide the tissue-specific biochemical information. Experimental data were acquired by numerical simulation with a digital brain phantom to compare the performance of the kinetics-induced filter in PET parametric imaging.

II. Materials and Methods

A. Brief Review of Bilateral Filter

Bilateral filter was originally proposed by Tomasi and Manduchi for 2D image processing [7]. Due to its good performance in noise reduction and edge preservation, bilateral filter has been successfully applied to biomedical image denoising [6,8,9]. Mathematically, bilateral filter can be written as follows:

$$\mathrm{BF}(x)(i) = \sum\nolimits_{j\in\mathcal{N}_i} w(i,j)x(j) \tag{1}$$

where $x(j)$ is the image intensity of voxel j, $\mathrm{BF}(x)(i)$ represents the restored intensity of voxel i, $\mathcal{N}_i$ enumerates the neighboring voxels centered at voxel i. The weight $w(i,j)$ consists of a product of two separate filters, one acting in the spatial domain, one acting in the intensity domain. Generally, the weight is designed with Gaussian shapes:

$$w(i,j) = \frac{1}{S(i)} \exp\left\{-\frac{(i-j)^2}{2\sigma_s^2}\right\} \exp\left\{-\frac{(x(i)-x(j))^2}{2\sigma_x^2}\right\} \tag{2}$$

where $S(i) = \sum_{j\in\mathcal{N}_i} \exp\{-\frac{(i-j)^2}{2\sigma_s^2}\} \exp\{-\frac{(x(i)-x(j))^2}{2\sigma_x^2}\}$ is a normalizing factor and two parameters σ_s and σ_x control spatial voxel neighborhood and image intensity similarity, respectively.

This work was partially supported by the National Natural Science Foundation of China under grand (No. 81000613, No. 81101046), the National Key Technology Research and Development Program of the Ministry of Science and Technology of China under grant (No. 2011BAI12B03), the Science and Technology Program of Guangdong Province of China under grant (No. 2011A030300005), National Key Scientific Instrument and Equipment Development Project of China under grant (No. 2011YQ03011404), and the 973 Program of China under grant (No. 2010CB732504). *Asterisk indicates corresponding author.*

Z. Bian, L. Lu, J. Ma, D. Zeng, Q. Feng, and W. Chen are with the School of Biomedical Engineering, Southern Medical University, Guangzhou 510515 China.

*J. Huang is with the School of Biomedical Engineering the Southern Medical University, Guangzhou 510515 China (telephone: 020-616-48285; e-mail: hjing@smu.edu.com).

B. Description of Kinetics-Induced Filter

In dynamic PET studies, voxels in physiologically similar regions should have similar tissue TAC kinetics. As a result, the tendency of TAC can provide tissue-specific biochemical information for dynamic PET image filtering. With this observation, in this paper, we propose a kinetics-induced filter to lower the noise of dynamic PET images by exploring the kinetic information.

Specifically, the present kinetics-induced filter is designed via the similarity between voxel-wise TACs under the framework of bilateral filter. Similar to Eq. (2), the weight of the kinetics-induced filter is constructed as:

$$\tilde{w}(i,j) = \frac{1}{\tilde{S}(i)} \exp\left\{-\frac{(i-j)^2}{2\sigma_s^2}\right\} \exp\left\{-\frac{\|Z(i)-Z(j)\|_W^2}{2\sigma_z^2}\right\} \quad (3)$$

where $\tilde{S}(i) = \sum_{j\in N_i} \exp\{-\frac{(i-j)^2}{2\sigma_s^2}\} \exp\{-\frac{\|Z(i)-Z(j)\|_W^2}{2\sigma_z^2}\}$ is a normalizing factor. The TAC at voxel k is denoted as $Z(k) = \{x(k,t), t = 1,2,\cdots,T\}$, where $k = i, j$ and T is the total sampling time frames. The similarity measure between two TACs is calculated by a norm $\|\cdot\|_W^2$, which is defined as $\|Y\|_W^2 = \sum_{t=1}^{T} W(t)Y^2(t)$, where W is the vector of weighting factors. A simple choice of W is $W = \{\triangle t_t\}$ where $\triangle t_t$ denotes the time duration of sampling frame t. Two parameters σ_s and σ_z control the spatial voxel neighborhood and the TAC similarity, respectively.

Based on the constructed weight $\tilde{w}(i,j)$, a voxel-wise weighted average operation can be performed for each frame, which is similar to Eq. (1). Thus the kinetics-induced filter can be described as follows:

$$\mathrm{KF}(x)(i,t) = \sum\nolimits_{j\in\mathcal{N}_i} \tilde{w}(i,j)x(j,t). \quad (4)$$

It is worth to notice that the average weights for the voxel i are same at each frame. Therefore, the kinetics-induced filter can also be performed to the noisy TACs directly as follows:

$$\mathrm{KF}(Z)(i) = \sum\nolimits_{j\in\mathcal{N}_i} \tilde{w}(i,j)Z(j). \quad (5)$$

From the weighted average of Eq. (5), we can see that the proposed kinetics-induced filter takes advantage of both the spatial and temporal consistencies of the dynamic PET data.

TABLE I

KINETIC PARAMETERS K_1, k_2, k_3, AND k_4 WITH THE UNIT OF MIN^{-1} USED IN THE ^{18}F-FDG PET SIMULATION.

Regions	K_1	k_2	k_3	k_4
Gray matter	0.1104	0.1910	0.1024	0.0094
White matter	0.0622	0.1248	0.0700	0.0097
Small tumor	0.0640	0.0890	0.0738	0.0057

C. Simulated Dynamic PET Studies

The present kinetics-induced filter was validated in a computer simulation. The tracer kinetic model used a dynamic ^{18}F-FDG study with a two-tissue compartment model for imaging glucose metabolism. In the simulation, a phantom which consists of gray matter, white matter and a small tumor inside the white matter [10] was used to simulate glucose metabolism in brain, as shown in Fig. 1(a). The TAC of each region was generated using a two tissue compartment model and an analytical blood input function in Feng's model [11], as shown in Fig. 1(b). The calculation of the kinetic model and the fitting procedure were performed using functions provided by the COMKAT package [12]. The kinetic parameters used in the simulation were taken from literature [13] and are listed in Table I. The fractional volume of blood in the tissue was set to zero for all regions. The scanning schedule of dynamic PET data consists of 30 time frames: 4×20 s, 4×40 s, 4×60 s, 4×180 s and 14×300 s, borrowed from the study [13]. In the simulation, the TACs were integrated for each frame and forward projected to generate dynamic sinograms and then Poisson noise was generated, which resulted in an expected total number of events over the 90 min equal to 50 million. The filtered back-projection (FBP) method with a ramp filter was used for the dynamic PET reconstruction.

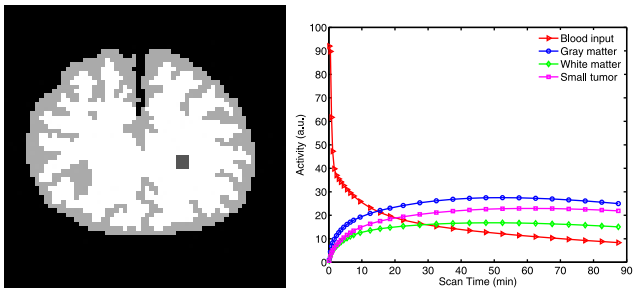

(a) (b)

Fig. 1. The ^{18}F-FDG PET simulation settings. (a) A brain phantom composed of gray matter, white matter and a small tumor; (b) The blood input function and regional time activity curves.

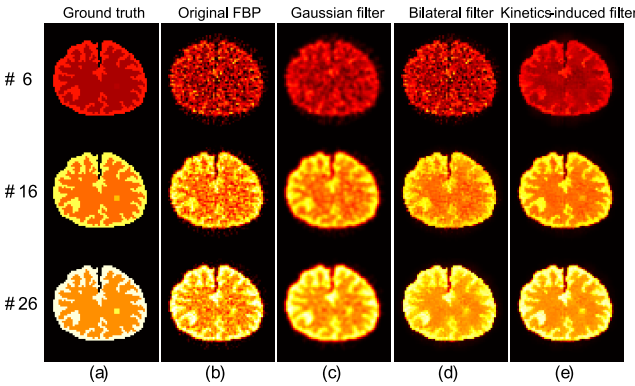

Fig. 2. The ground truth and the activity images reconstructed by different methods at frames #6, #16, and #26 (top to bottom). (a) are the ground truth; (b) are from the direct FBP reconstruction; (c) are from the FBP images processed by a Gaussian filter with the standard deviation $\sigma_g = 0.9$; (d) are from the FBP images processed by the bilateral filter with $\sigma_s = 4$ and $\beta = 0.5$; and (e) are from the FBP image processed by the present kinetics-induced filter with $\sigma_s = 4$ and $\sigma_z = 20$. All images are with same display window.

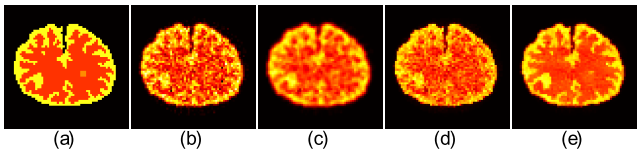

Fig. 3. The ground truth and the K_i images estimated by different methods: (a) is the ground truth; (b) is from the direct FBP reconstruction; (c) is from the FBP images processed by a Gaussian filter with the standard deviation $\sigma_g = 0.9$; (d) is from the FBP images processed by the bilateral filter with $\sigma_s = 4$ and $\beta = 0.5$; and (e) is from the FBP image processed by the present kinetics-induced filter with $\sigma_s = 4$ and $\sigma_z = 20$. All images are with same display window.

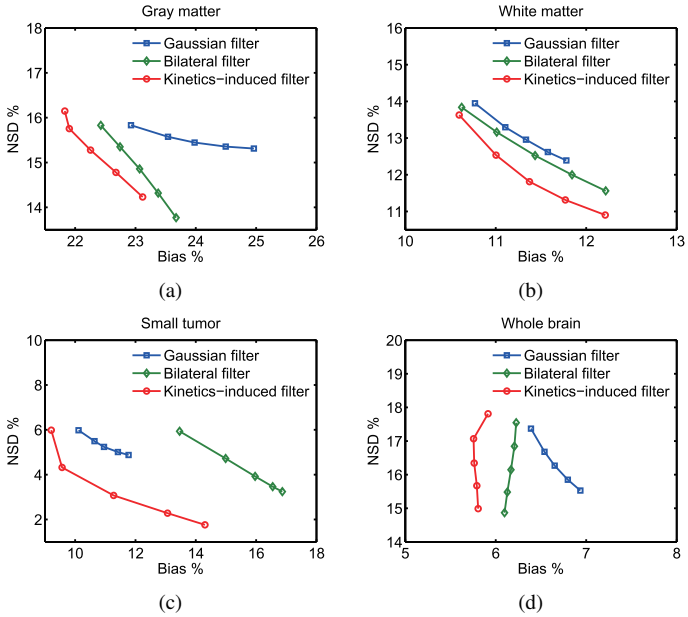

Fig. 4. The NSD versus Bias tradeoff curves of the influx rate K_i images estimated from the FBP images processed by the Gaussian filter, bilateral filter and kinetics-induced filter in different brain regions. Different points on the curves were obtained by varying the parameters σ_g, β and σ_z, respectively.

III. Results

To evaluate the performance of the present kinetics-induced filter, the conventional Gaussian filter and bilateral filter were selected for comparison. Because the parameter σ_x for bilateral filter should vary with different frames, alternatively, we propose the following frame-dependent parameter written as $\sigma_{x,m} = \beta\sigma_m$, where β is a scaling factor, and σ_m is the estimated variance for frame m, which is the same as that used in our previous work [14]. For all these cases, a $\mathcal{N}_i = 7\times 7$ window centered at each voxel was used for the neighbor averaging.

A. Comparison of Dynamic PET Activity Images

Figure 2 shows the ground truth and the activity images reconstructed by different methods at the frames #6, #16, and #26. The rows from top to bottom show the results at frames #6, #16, and #26, respectively, i.e., the first column images represent the ground truth; the second column are the results from the direct FBP reconstructions; and the third column images are the results from the FBP image processed by a Gaussian filter with the standard deviation $\sigma_g = 0.9$; the fourth column images are the results from the FBP image processed by the bilateral filter with $\sigma_s = 4$ and $\beta = 0.5$; and the fifth column images are the results from the FBP image processed by the present kinetics-induced filter with $\sigma_s = 4$ and $\sigma_z = 20$. The results demonstrate that the present kinetics-induced filter method can yield significant noise reduction without suffering edges and concealing subtle information as comparison to other methods.

B. Comparison of PET Parametric Images

In the ^{18}F-FDG PET studies, a major parameter of interest is the influx rate $K_i = K_1k_3/(k_2 + k_3)$, which is related to the glucose metabolic rate by a scaling factor. Figure 3 shows the ground truth and the K_i images estimated from different methods: (a) is the ground truth; (b) is from the direct FBP reconstruction; (c) is from the FBP image processed by the Gaussian filter with the standard deviation $\sigma_g = 0.9$; (d) is from the FBP image processed by the bilateral filter with $\sigma_s = 4$ and $\beta = 0.5$; and (e) is from the FBP image processed by the present kinetics-induced filter with $\sigma_s = 4$ and $\sigma_z = 20$. It can be seen that the present kinetics-induced filter can achieve a better performance than other methods in terms of both the noise reduction and detailed K_i parametric information preservation.

In order to quantitatively evaluate the performance of the present kinetics-induced filter, we use quantitative evaluation criteria involving regional Normalized Standard Deviation (NSD) versus Bias tradeoff curves. Borrowing the definitions in [14], the NSD and Bias are defined as:

$$\mathrm{NSD}_{\mathrm{roi}} = \frac{\sqrt{\frac{1}{|M_{\mathrm{roi}}|-1}\sum_{j\in M_{\mathrm{roi}}}\left(K_i(j) - \bar{K}_{\mathrm{roi}}\right)^2}}{\bar{K}_{\mathrm{roi}}} \times 100\% \quad (6)$$

$$\mathrm{Bias}_{\mathrm{roi}} = \frac{\left|\bar{K}_{\mathrm{roi}} - K^{\mathrm{true}}_{\mathrm{roi}}\right|}{K^{\mathrm{true}}_{\mathrm{roi}}} \times 100\% \quad (7)$$

where $K_i(j)$ denotes the estimated K_i parametric value at a voxel $j (j = 1, 2, \cdots, |M_{\mathrm{roi}}|)$ of the specified ROI, $\bar{K}_{\mathrm{roi}} = \sum_{j\in M_{\mathrm{roi}}} K_i(j)/|M_{\mathrm{roi}}|$ denotes the mean value of estimated K_i parametric value in the specified ROI, M_{roi} enumerates all the voxels in the specified ROI, and $|M_{\mathrm{roi}}|$ represents the number of voxel in the specified ROI. For the regional bias ($\mathrm{Bias}_{\mathrm{roi}}$), $K^{\mathrm{true}}_{\mathrm{roi}}$ is the known uniform parametric value in the given ROI.

Figure 4 shows NSD versus Bias tradeoff curves of the influx rate K_i estimated from Gaussian filter method, bilateral filter method and the present kinetics-induced filter method for different regions in the brain phantom. Different points on the curves were obtained by varying the parameters σ_g, β and σ_z, respectively. It can be seen that parametric images generated from the restored dynamic activity images with our proposed filter performs better in terms of NSD versus Bias tradeoff analysis than those generated by the other two methods.

IV. Discussion and Conclusion

To improve the quantitative accuracy of parametric imaging, it is necessary to reduce the noise of the dynamic PET images. Recently, for this purpose, bilateral filter has been investigated in PET studies with significant gains than Gaussian filter in terms of the noise reduction and resolution preservation [6]. However, as one type of spatial filters, bilateral filter just reduce the noise in individual frames without considering the kinetic information contained within all the dynamic images. Therefore, in this paper, aiming to improve the quantitative accuracy of parametric imaging, we developed a kinetics-induced filter to lower the noise of dynamic PET images by exploring the kinetic information. The present kinetics-induced filter is designed via the similarity between voxel-wise TACs under the framework of bilateral filter. The smoothing is controlled by the both the geometric closeness and the kinetics similarity between the center voxel of the neighborhood and a nearby voxel in the neighborhood. We have performed the simulation studies to validate and evaluate the present kinetics-induced filter. The results indicate that the present kinetics-induced filter can achieve better bias-variance properties and quantitative accuracy for parametric images than the conventional Gaussian filter and bilateral filter.

In addition to the image post-processing techniques, many statistical iterative reconstruction methods have also been explored to reduce the noise of the dynamic PET images [15-18]. Usually, prior information is used under the maximum a posteriori (MAP) reconstruction framework, i.e., anatomical similarity information from high-resolution MR or CT images [15], temporal information from kinetic models [16] and local image structure information [17,18]. Considering its remarkable performance in the noise reduction, the present kinetics-induced filter could be modified as a spatio-temporal prior of MAP reconstruction for dynamic PET.

Similar to bilateral filter, a difficult task for performing the present kinetics-induced filter is the parameter selections including the size of the neighbor window, and the smoothing parameters which control the geometric closeness and the kinetics similarity, respectively. In this study, all the parameters were determined by trial-and-error fashion and visual inspection. In practice, all parameters should be optimized adaptively based on the special application cases [19,20].

In the future, applying the present kinetics-induced filter to clinical dynamic PET studies to validate its effectiveness, and exploring some kind of methodology for the parameters selection would be useful and interesting topics.

References

[1] M. E. Phelps, *PET: molecular imaging and its biological applications*. Springer, New York 2004.

[2] R. N. Gunn, A. A. Lammertsma, S. P. Hume, and V. J. Cunningham, "Parametric imaging of ligand-receptor binding in PET using a simplified reference region model," *NeuroImage*, vol. 6, no. 4, pp. 279-287, 1997.

[3] J. M. Links, J. P. Leal, H. W. Mueller-Gaertner, and H. J. Wagner, "Improved positron emission tomography quantification by Fourier-based restoration filtering," *Eur J Nucl Med*, vol. 19, no. 11, pp. 925-932, 1992.

[4] J. W. Lin, A. F. Laine, and S. R. Bergmann, "Improving PET-based physiological quantification through methods of wavelet denoising," *IEEE Trans Biomed Eng*, vol. 48, no. 2, pp. 202-212, 2001

[5] H. C. So, S. L. Jae, S. L. Dong, and S. P. Kwang, "Noise reduction of parametric images of myocardial blood flow by filtering $H_2{}^{15}O$ dynamic PET images using wavelet transform," in *Proc. IEEE NSS*, 2002, pp. 1341-1343.

[6] F. Hofheinz, J. Langner, B. Beuthien-Baumann, L. Oehme, J. Steinbach, and J. Kotzerke, *et al.*, "Suitability of bilateral filtering for edge-preserving noise reduction in PET," *EJNMMI Res*, vol. 1, no. 1, pp. 23, 2011.

[7] C. Tomasi and R. Manduchi, "Bilateral filtering for gray and color images," in *Proc. ICCV*, 1998, pp. 839-846.

[8] J. C. Kosior, R. K. Kosior, and R. Frayne, "Robust dynamic susceptibility contrast MR perfusion using 4D nonlinear noise filters," *J Magn Reson Imaging*, vol. 26, no. 6, pp. 1514-1522, 2007.

[9] S. Balocco, C. Gatta, O. Pujol, J. Mauri, and P. Radeva, "SRBF: Speckle reducing bilateral filtering," *Ultrasound Med Biol*, vol. 36, no. 8, pp. 1353-1363, 2010.

[10] G. Wang and J. Qi, "Generalized algorithms for direct reconstruction of parametric images from dynamic PET data," *IEEE Trans Med Imaging*, vol. 28, no. 11, pp. 1717-1726, 2009.

[11] D. Feng, K. P. Wong, C. M. Wu, and W. C. Siu, "A technique for extracting physiological parameters and the required input function simultaneously from PET image measurements: theory and simulation study," *IEEE Trans Inf Technol Biomed*, vol. 1, no. 4, pp. 243-254, 1997.

[12] R. J. Muzic and S. Cornelius, "COMKAT: compartment model kinetic analysis tool," *J Nucl Med*, vol. 42, no. 4, pp. 636-645, 2001.

[13] F. O'Sullivan and A. Saha, "Use of ridge regression for improved estimation of kinetic constants from PET data," *IEEE Trans Med Imaging*, vol. 18, no. 2, pp. 115-125, 1999.

[14] L. Lu, N. A. Karakatsanis, J. Tang, W. Chen, and A. Rahmim, "3.5D dynamic PET image reconstruction incorporating kinetics-based clusters," *Phys Med Biol*, vol. 57, no. 15, pp. 5035-5055, 2012.

[15] L. Lu, J. Ma, J. Huang, H. Zhang, Z. Bian, and W. Chen, *et al.*, "Generalized metrics induced anatomical prior for MAP PET image reconstruction," in *Fully3D*, 2011, pp. 233-236.

[16] Z. Bian, J. Ma, J. Huang, H. Zhang, L. Lu, and Q. Feng, *et al.*, " Regional spatio-temporal prior based dynamic PET reconstruction," in *Fully3D*, 2011, pp. 407-410.

[17] L. Tian, J. Ma, Z. Liang, J. Huang, and W. Chen, "Information divergence constrained total variation minimization for positron emission tomography image reconstruction," in *Proc. IEEE NSS-MIC*, 2011, pp. 2587-2592.

[18] J. Ma, Q. Feng, Y. Feng, J. Huang, and W. Chen, "Generalized Gibbs priors based positron emission tomography reconstruction," *Comput Biol Med*, vol. 40, no. 6, pp. 565-571, 2010.

[19] J. Ma, J. Huang, Q. Feng, H. Zhang, H. Lu, and Z. Liang, *et al.*, "Low-dose computed tomography image restoration using previous normal-dose scan," *Med Phys*, vol. 38, no. 10, pp. 5713-5731, 2011.

[20] J. Ma, H. Zhang, Y. Gao, J. Huang, Z. Liang, and Q. Feng, *et al.*, "Iterative image reconstruction for cerebral perfusion CT using a pre-contrast scan induced edge-preserving prior," *Phys Med Biol*, vol. 57, no. 22, pp.7519-7542, 2012.